

## CHAPTER 276

# On validation of a sand waves and sand banks model

S. J. M. H. Hulscher \*

### Abstract

A morphological model is described for the interaction between tidal motion and an erodible bed. This model is able to distinguish between a flat bed, and the generation of tidal sand banks and/or sand waves, based on physical parameters. The physical meaning of the turbulence parameters  $A_v$  and  $S$ , as used in this model is subject of discussion in the present paper, therefore a simpler system is investigated. A simple flow is described by a logarithmic profile model (a generally accepted turbulence model), as well as by a partial slip model, using  $A_v$  and  $S$ . It is shown that the two models can be calibrated such that they produce the same bed shear stress, depth-averaged velocity and depth-averaged eddy viscosity. This leads to expressions for  $A_v$  and  $S$  as function of the roughness height and a shape parameter in the logarithmic profile model. Application of this information to two locations shows that the bed form prediction model gives encouraging results.

## 1 Introduction

The offshore seabed of shallow seas is covered with rhythmic patterns on a large scale, see e.g. *Off* [1963]. Tidal sand banks have wavelengths of about five kilometers and reach heights up to 40 meters. Sand waves, see figure 1 are smaller, wavelengths of 500 meters, heights up to 10 meters. Both patterns are shown in a schematic way in figure 2. When these two patterns overlap, the crests are oriented differently (angle between  $60^\circ$ -  $90^\circ$ ), which suggests that these two patterns

---

\*Civil Engineering & Management, University of Twente, P.O. box 217, 7500 AE, Enschede, The Netherlands.

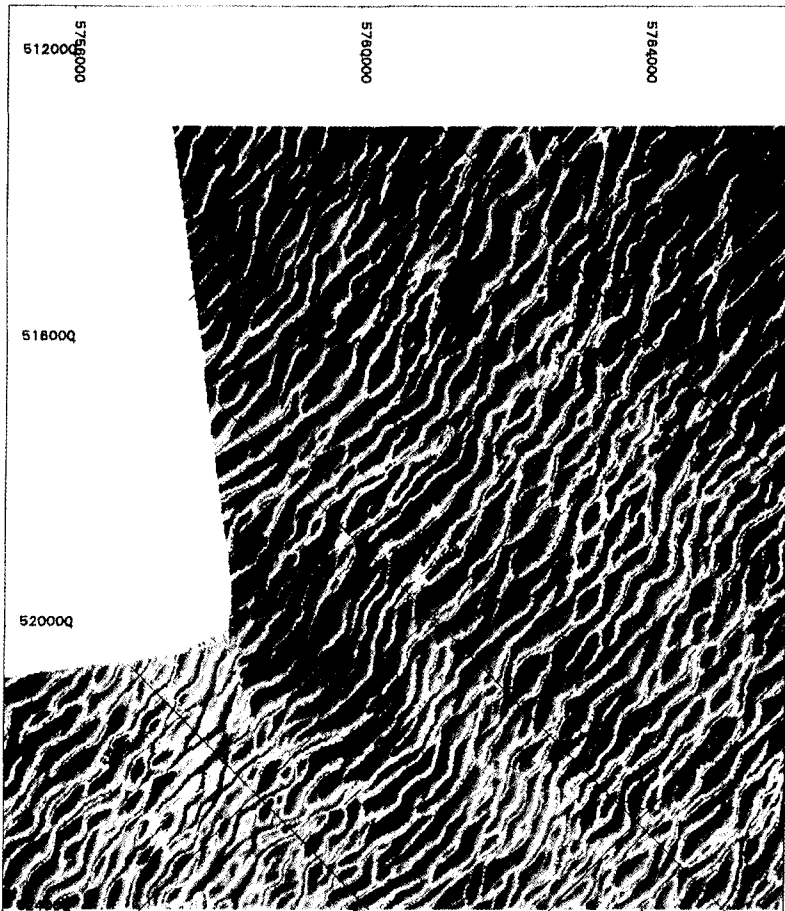


Figure 1: *Visualization of the North Sea bed near the Eurogeul, from Van Goor & Andorka Gal, 1996.*

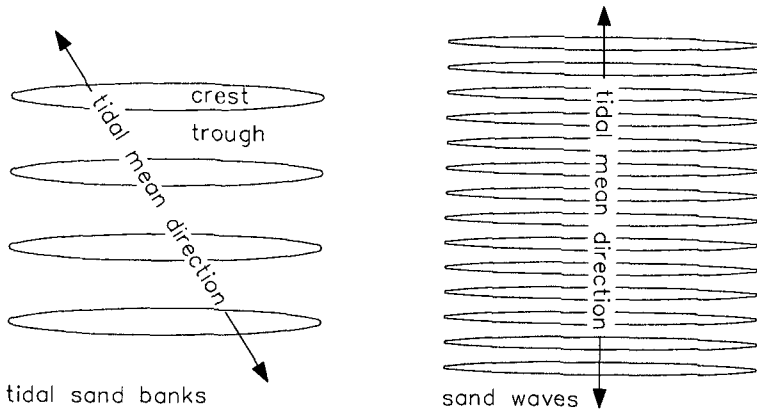


Figure 2: Sketch of tidal sand banks and sand waves, the relation to the main tidal current axis is indicated.

are different. Therefore different mechanisms are responsible for their formation and behavior.

A model to describe formation of these large-scale sea-bed patterns due to tide-topography interactions is given in *Hulscher* [1996]. In this model the tide is described by a three-dimensional shallow water model. This model uses a very simple turbulence closure scheme, see also *Engelund* [1970]: constant eddy viscosity  $A_v$  in combination with a partial slip parameter at the bottom. The latter introduces a so-called resistance parameter  $S$ .

Application of this turbulence model often raises questions how these results compare with more realistic turbulence-closure schemes. Unfortunately it is not completely known how turbulence should be modeled, therefore the answer to this question can never be definite. A further, even more important question is how these, rather abstract, parameters can be determined from observations. Illustrative issue is whether observations are to be collected either on the top and in the trough of the bank or at the adjacent sides.

A start to answer the first question is made studying a simplified system: a two-dimensional horizontal model without Coriolis force and neglecting inertia effects. This system is analyzed in two ways: using a realistic turbulence closure scheme and the simple scheme based on eddy viscosity and the resistance parameter. By comparing the results of these two methods one finds explicit relations between at one hand more accepted model parameters and at the other hand, the eddy viscosity  $A_v$  and the resistance parameter  $S$ . Furthermore this enables to investigate how the latter two variables are connected, and if they represent two degrees of freedom.

These results can be used to make estimates for the three dimensional model in which Coriolis effects and inertia effects are included. These lead to choices for the parameters which are following *Hulscher* [1996] crucial to determine the

bed structure: a flat bed or sand waves or tidal sand banks or a combination of the latter two patterns. This procedure enables the estimate of these parameters without analyzing an network of current meter recordings. For two cases explicit estimates are given: an average North Sea location and the Middelkerke bank.

The outline of this note is as follows. A short description of the three-dimensional bed form model is given in section 2. Next, the simplified system and subsequent modeling is given in section 3. The analyses in particular for the logarithmic profile and the  $A_v - \hat{S}$  model are given in sections 3.3 and 3.4, respectively. Matching of these two models is discussed in section 3.5. These results are transferred to the three dimensional model, which is shown and discussed in section 4. In this section two physical locations are treated as examples. Lastly, conclusions are presented in section 5.

## 2 Model for sand waves and tidal sand banks

The generation of large-scale bed form patterns is studied based on the idea that these structures might be free instabilities of the coupled morphological system: sea water and sea bed. Therefore a suitable model of this system is formulated and use for analysis.

The morphological shallow water is based on tidal flow described by three-dimensional shallow water equations, bed load transport and conservation of sediment. Tidal averaging and application of a linear stability analysis lead to prediction of the dominant bottom mode starting from a flat bottom. Translating the measures of these fastest growing sinusoidal sea bed waves into physical quantities shows that the pattern is similar to either similar to sand waves or to tidal sand banks; patterns which are significantly different, see figure 2. This leads to the qualitative result in figure 3; the derivation of this figure is described in detail in *Hulscher* [1996].

Figure 3 shows that the bed structure prediction depends strongly on the Stokes number  $E_v$  of the tidal flow and the bed resistance parameter  $\hat{S}$ . These are defined as

$$E_v = \frac{2A_v}{H^2\sigma} \quad \text{and} \quad \hat{S} = \frac{2S}{H\sigma}, \quad (1)$$

in which  $H$  is the local mean depth and  $\sigma$  the frequency of the tidal motion. The constant turbulent eddy-viscosity,  $A_v$  ( $m^2s^{-1}$ ), quantifies the way in which horizontal momentum is transferred in vertical direction. The quantity  $S$  ( $ms^{-1}$ ) is used to model the partial slip near the bed boundary. This overcomes the problem that the constant eddy viscosity is near the bottom too simple to model both velocity and shear stress in a realistic way. After *Engelund* [1970] here  $A_v$  and  $S$  are considered as two constants which describe together the vertical profile of the vertical flow profile.

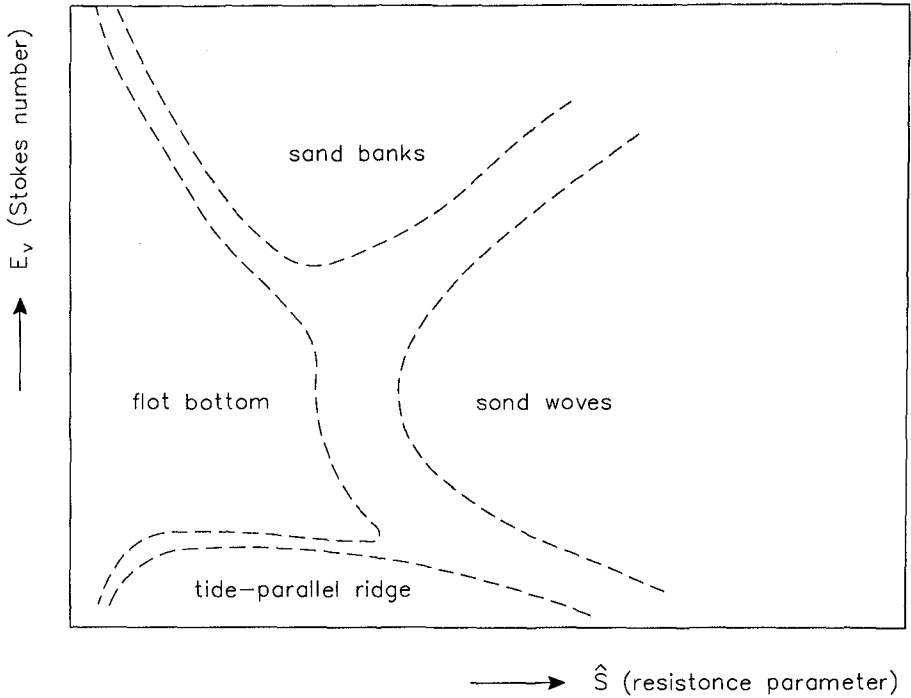


Figure 3: *Characteristic bed forms predicted by the three-dimensional shallow water model as a function of the bottom slip parameter  $\hat{S}$  and the Stokes number  $E_v$ . Quantification depends on values of the Coriolis parameter, local depth, bed-slope effects on sediment transport and the nonlinearity in the bedload transport formula.*

### 3 Modelparameter derivation

#### 3.1 Simplified situation model

To illustrate the procedure a very simplified model and model-situation is sufficient. Starting from the three-dimensional shallow water model as in *Hulscher* [1996] the simplifications are as follows:

- Coriolis effects are neglected
- tidal flow,  $\tilde{u}(z, t)$ , is horizontally uniform
- friction dominates inertia effects: the eddy turn-over scale is much smaller than the scale on which the flow varies, such that eddies can reach a statistical equilibrium

Here the tidal flow is driven by pressure gradient, oscillating at the tidal frequency  $\sigma$  and having amplitude  $P_x$ . The flow is opposite the pressure gradient; the equation of motion becomes

$$0 = -\frac{P_x}{\rho} \sin \sigma t + \frac{\partial}{\partial z} \left[ \nu_t(z, t) \frac{\partial \tilde{u}}{\partial z} \right], \quad (2)$$

in which  $\nu_t$  is the turbulent eddy viscosity coefficient. The boundary conditions near the sea bed and surface are as follows

$$\begin{aligned} \tilde{u} &= 0 & \text{at } z &= z_0, & (3) \\ \nu_t(z, t) \frac{\partial \tilde{u}}{\partial z} &= 0 & \text{at } z &= H, & (4) \end{aligned}$$

in which  $z_0$  is the roughness height. The  $z$ -axis is here directed upwards, from the sea bottom  $z = 0$  till the sea surface  $z = H$ . Here the surface stress component is chosen zero. The bottom shear stress is denoted by  $\tilde{\tau}_b(t)$  and is time-dependent:

$$\tilde{\tau}_b = \rho \nu_t(z) \frac{\partial \tilde{u}}{\partial z} \equiv \rho |\tilde{u}_*| \tilde{u}_* \quad \text{at } z = 0, \quad (5)$$

where  $\tilde{u}_*$  is the time-dependent friction velocity.

##### 3.1.1 Linearization of the shear stresses

Definition (5) shows that, in general, the friction velocity  $\tilde{u}_*$  depends on time, so that the momentum equation is difficult to solve. To deal with this one usually replaces one friction velocity factor  $\tilde{u}_*$  by a representative constant  $\bar{u}_*$ . Now the bed shear stress condition becomes

$$\tilde{\tau}_b = \rho \nu_t(z) \frac{\partial \tilde{u}}{\partial z} \equiv \rho \bar{u}_* \tilde{u}_* \quad \text{at } z = 0, \quad (6)$$

A possible way to derive such a representative value for  $\bar{u}_*$  is requiring that the tidal-averaged shear stresses of both formulations are equal:

$$\rho \langle \tilde{u}_* \tilde{u}_*^2 \rangle = \rho \langle \bar{u}_* \hat{u}_*^2 \rangle, \quad (7)$$

in which  $\langle \rangle$  denotes the tidal averaging. Further assuming that the friction velocity oscillates with the tidal frequency  $\sigma$  (like the forcing pressure gradient) and that it has an amplitude  $\hat{u}_*$ , the searched constant becomes [Zimmerman, 1981, and Mei, 1989]

$$\bar{u}_* = \frac{8}{3\pi} \hat{u}_*. \quad (8)$$

### 3.2 Model analysis: general part

In this model the tidal flow is forced by the pressure gradient and as the latter oscillates at frequency  $\sigma$ , so in absence of inertia effects the tidal flow can simply be decomposed as follows

$$\tilde{u}(z, t) = u(z) \sin(\sigma t). \quad (9)$$

Substitution of (9) into the equation (2) leads to the following equation of motion for  $u(z)$ :

$$0 = -\frac{P_x}{\rho} + \frac{\partial}{\partial z} \left[ \nu_t(z) \frac{\partial u}{\partial z} \right]. \quad (10)$$

By integration of (10) using the upper boundary condition (4) and the lower as given in (6), the following equality is obtained

$$\frac{P_x}{\rho} H = \bar{u}_* \hat{u}_* = \frac{8}{3\pi} \hat{u}_*^2. \quad (11)$$

Up till this point no simplifications are made regarding the choice of a specific turbulence closure scheme. In the next two sections equation (10) will be solved using two different turbulence closure schemes.

### 3.3 Logarithmic profile model and analysis

**Viscosity parametrization** From turbulence modelling is known that the turbulent eddy viscosity increases from the boundaries in which the distance to the boundary is a measure for the length scale of the turbulent eddies. So at the fixed sea bottom the eddy viscosity equals zero and it increases with the distance from the bottom  $z$ :

$$\nu_t(z) \sim z. \quad (12)$$

The sea surface can act as a less stringent boundary. Many physical processes lead to a more effective mixing in the upper part of the water column, e.g. action

of wind waves, swell, stratification. Here this fact is parametrized by a parameter  $\epsilon$ , which value is here between the limits 1/2 (little influence of surface on turbulence) and 1 (rigid surface). This is chosen such that the viscosity at the sea surface is:

$$\nu_t(H) \sim H(1 - \epsilon). \quad (13)$$

And near the surface  $H - \zeta$  (in which  $\zeta$  positive) the length scale of the turbulent eddies increases following

$$\nu_t(H - \zeta) \sim \nu_t(H) + \zeta(2\epsilon - 1). \quad (14)$$

The previous considerations motivate a parabolic function as parametrization for the dimensional turbulent eddy viscosity  $\nu_t$

$$\nu_t(z) = k\hat{u}_*z \left(1 - \epsilon \frac{z}{H}\right), \quad (15)$$

in which  $\kappa$  is the Von Karman constant  $\kappa \simeq 0.41$ .

**Velocity profile** Solving equation (10), using boundary conditions (3), (4) and expressing it in terms of  $\bar{u}_*$  using (6) yields

$$u(z) = \frac{\bar{u}_*}{\kappa} \left[ \ln\left(\frac{z}{z_0}\right) + \frac{(1 - \epsilon)}{\epsilon} \ln\left(\frac{1 - \epsilon \frac{z}{H}}{1 - \epsilon \frac{z_0}{H}}\right) \right]. \quad (16)$$

**Depth-averaged quantities** The depth-average value of the turbulent eddy viscosity can easily be computed from equation (15) and yields

$$\bar{\nu}_t = k\hat{u}_*H \frac{(3 - 2\epsilon)}{6}. \quad (17)$$

In figure 4 the normalized viscosity profile is shown. The depth-averaged velocity follows from equation (16) and is given by

$$\bar{u} = \frac{\bar{u}_*}{\kappa} \left[ \ln\left(\frac{H}{z_0}\right) - \frac{1}{\epsilon} + \frac{1 - \epsilon}{\epsilon} \ln\left(\frac{1 - \epsilon}{1 - \epsilon \frac{z_0}{H}}\right) + \frac{\epsilon - 1}{\epsilon^2} \ln(1 - \epsilon) \right]. \quad (18)$$

### 3.4 $A_v - S$ model

In this section the highly simplified turbulence model is chosen, here called  $S$  and  $A_v$  model, which is applied in *Hulscher* [1996]). The model has a vertically constant eddy viscosity, here denoted by  $A_v$ . This constant eddy viscosity model lacks variations which lead to describe the correct velocity and shear stress both in the interior as well as at the bottom. However, the aim here is to use this model for studying sediment transport, therefore it has to produce the correct bed shear stress, rather than the exact horizontal velocity near the sea bed. This can be achieved by choosing a partial slip condition, instead of condition (3), at the sea bed. In this context the partial slip condition is formulated as follows

$$\bar{u}_* \hat{u}_* = Su \quad \text{at} \quad z = 0, \quad (19)$$

in which  $S$  is the so-called resistance parameter.

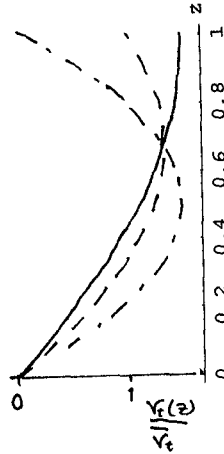


Figure 4: The dimensionless viscosity profile  $\nu_t(z)/\bar{\nu}_t$  for three values of  $\epsilon$  (straight  $\epsilon = 0.5$ , dashed/dotted  $\epsilon = 0.75$ , dashed  $\epsilon = 1.0$ ).

**Velocity profile** The solution of equation (2), using (4) and (19) becomes

$$u(z) = \bar{u}_* \hat{u}_* \left[ \frac{z}{A_v} \left( 1 - \frac{z}{2H} \right) + \frac{1}{S} \right]. \quad (20)$$

**Depth-averaged quantities** The depth-averaged viscosity in this model is simply the constant

$$\bar{\nu}_t = A_v. \quad (21)$$

The depth-averaged velocity  $\bar{u}$  in this model yields

$$\bar{u} = \bar{u}_* \hat{u}_* \left( \frac{H}{3A_v} + \frac{1}{S} \right). \quad (22)$$

### 3.5 Matching

Now the models, discussed in the previous two sections, section 3.3 and section 3.4, will be matched by appropriate requirements. First remark is that sediment transport is a function of the bed shear stress. This motivates the first requirement: the  $A_v - S$  model has to produce the same bottom shear stress as in the logarithmic model. Based on this, the bottom boundary condition in the  $A_v - S$  model has already been adapted such that expression (6) is valid in both models.

The second condition is that the water discharge is equal in both models. This condition is here transferred into the requirement of equal depth-averaged velocities resulting from both turbulence formulations. Using equations (18) and (22) this means

$$\ln \left( \frac{H}{z_0} \right) - \frac{1}{\epsilon} + \frac{1-\epsilon}{\epsilon} \ln \left( \frac{1-\epsilon}{1-\epsilon \frac{z_0}{H}} \right) + \frac{\epsilon-1}{\epsilon^2} \ln(1-\epsilon) = \kappa \hat{u}_* \left( \frac{H}{3A_v} + \frac{1}{S} \right). \quad (23)$$

The third condition is that the depth-averaged value of the eddy viscosity  $\bar{\nu}_t$  equals the constant eddy viscosity  $A_v$ . Using equation (17) this leads to

$$A_v = k\hat{u}_*H\frac{(3-2\epsilon)}{6}. \quad (24)$$

## 4 Discussion

Before the discussion here starts, it is worthwhile to remark that all values for turbulent eddy viscosity coefficients and bottom shear stress are results of the application of a turbulence closure scheme. The logarithmic model, used as a reference here, is often applied and produces satisfactory results. Therefore this model is generally accepted.

In the present model this leads to the following Stokes number  $E_v$  by using equations (11) and (24)

$$E_v = \frac{\kappa\sqrt{\frac{3\pi P_x H}{8\rho}}}{H\sigma} \left(1 - \frac{2}{3}\epsilon\right). \quad (25)$$

So if  $P_x, H, \sigma$  are already determined, the value of  $E_v$  is still a function of  $\epsilon$ .

Using equations (11), (24) and the matching condition (23) the following relation for  $\hat{S}$  and  $E_v$  is obtained

$$\frac{E_v}{\hat{S}} = \frac{3-2\epsilon}{6} \left[ \ln\left(\frac{H}{z_0}\right) - \frac{1}{\epsilon} + \frac{1-\epsilon}{\epsilon} \ln\left(\frac{1-\epsilon}{1-\epsilon\frac{z_0}{H}}\right) + \frac{\epsilon-1}{\epsilon^2} \ln(1-\epsilon) \right] - \frac{1}{3} \quad (26)$$

This relation shows that  $\hat{S}$  is a function of the roughness height  $z_0$ , if the other parameters are specified. As  $z_0$  usually is between  $5 \cdot 10^{-5}$  m and  $2 \cdot 10^{-1}$  m and  $\frac{1}{2} \leq \epsilon \leq 1$ , this will restrict the values of  $E_v, \hat{S}$  which are physically relevant.

### 4.1 Physical discussion

In general, the pressure gradient  $P_x$  can be determined from observations. Here the pressure gradient  $P_x$  is roughly estimated from the  $M_2$  tidal (spring) range  $\Delta$ , following

$$P_x = \rho * g * \frac{2\Delta}{L}, \quad (27)$$

in which  $L$  is the tidal wavelength and  $g$  the gravity acceleration. Assuming that  $\Delta$  is 2 meters and the tidal wave follows from shallow water theory (so  $L=770$  kilometers on a depth of 30 meters) one derives  $P_x = \rho * 5.1 \cdot 10^{-5} \text{ms}^{-2}$ ; the tidal frequency is  $\sigma = 1.4 \cdot 10^{-4} \text{s}^{-1}$ .

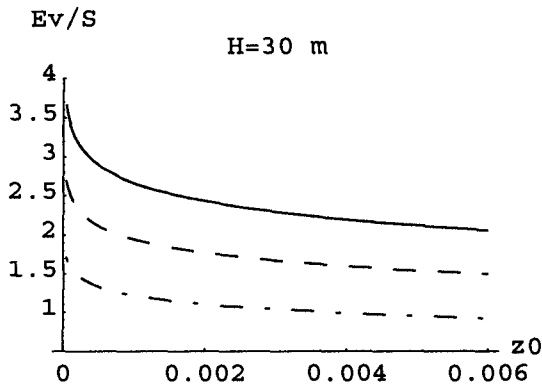


Figure 5: (a) The ratio  $E_v/\hat{S}$  and (b)  $\hat{S}$  for three values of  $\epsilon$  (straight  $\epsilon = 0.5$ , dashed/dotted  $\epsilon = 0.75$ , dashed  $\epsilon = 1.0$ ). Here average North Sea conditions are chosen, the depth  $H = 30$  meters.

**Offshore North Sea** A suitable North Sea average depth is 30 m. Using equation (25) gives that  $1.4 \leq E_v \leq 2.8$  due to the range of  $0.5 \leq \epsilon \leq 1$ . The correct value of  $\epsilon$  has to be estimated based on current profiles. Using many field measurements *Sousby* [1990] has found that the roughness height  $z_0$  in the North sea usually is between  $5 \cdot 10^{-5}$  m and  $6 \cdot 10^{-3}$  m, in which the larger values are found for rippled sand. Using (26) the ratio  $E_v/\hat{S}$  and subsequently the resistance parameter itself can be evaluated. Figure 5(a) shows the ratio  $E_v/\hat{S}$  and in figure 5(b) the resistance parameter  $\hat{S}$  is shown.

**Middelkerke Bank** The Middelkerke Bank is part of the Flemish Banks system; these large tidal sand banks are partly covered with sand waves. At the Middelkerke Bank the mean depth is significantly smaller, being about 15 meters. So here the expected range for the Stokes number becomes  $2.0 \leq E_v \leq 3.9$ . *Vincent & Stolk* [1993], p 217, reported that the roughness height  $z_0$  at two stations around the Middelkerke Bank is between  $9 \cdot 10^{-4}$  m and  $3.3 \cdot 10^{-2}$  m. For these values the ratio  $E_v/\hat{S}$  and the resistance parameter  $\hat{S}$  are shown in figure 6.

**General** The areas in parameter space of both discussed locations are shown in figure 7. In this figure also the expected bed structure based on the bed form prediction model *Hulscher* [1996] is also indicated. For the offshore North Sea bed a part of the possible parameter combinations predict a flat sea bed, also a part of these combinations predicts tidal sand banks. Around the Middelkerke bank a part of the parameter combinations predicts tidal sand banks, for a different part the slowly growing tidal sand banks are dominated by sand waves, which grow faster. Comparison between prediction and the actual bed structure show that these results are not unrealistic. So the ranges in the parameters  $E_v$  and  $\hat{S}$

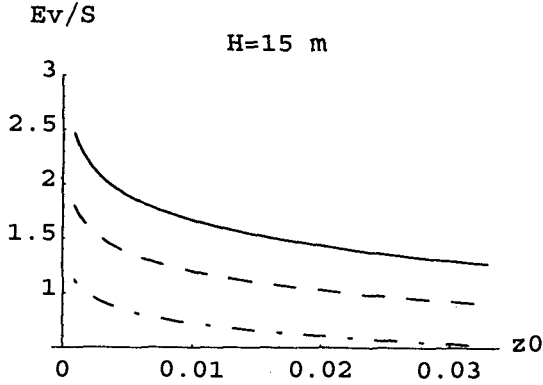


Figure 6: (a) The ratio  $E_v/\hat{S}$  and (b)  $\hat{S}$  for three values of  $\epsilon$  (straight  $\epsilon = 0.5$ , dashed/dotted  $\epsilon = 0.75$ , dashed  $\epsilon = 1.0$ ). Here Middelkerke Bank conditions are chosen, the depth  $H = 15$  meters.

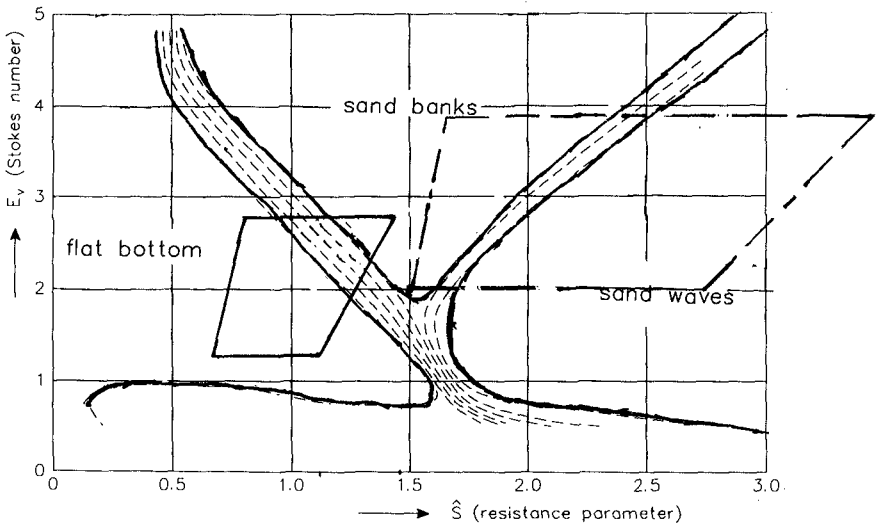


Figure 7: Parts of the parameter space  $E_v$  and  $\hat{S}$  possible in the offshore North Sea bed and around the Middelkerke bank. Also the expected bed behavior as found by Hulscher [1996] is indicated.

based on natural variations in the quantities roughness height  $z_0$  and turbulence characteristics  $\epsilon$  cover different bed structures. These results show that it will be worthwhile to determine the value of  $z_0$  and  $\epsilon$  more precise and subsequently compare the model prediction with the observed local bed structure, for several locations in the North Sea.

## 5 Conclusions

A way to investigate the implication of a potential sea-bed prediction model is presented. To quantify the parameters which describe the turbulence processes, first a simpler system, based on steady flow, is analyzed.

In the simpler system is shown that the  $S, A_v$ -turbulence model is able to produce the same bed shear stress as the accepted logarithmic model. The comparison between these models gives expressions for  $S$  and  $A_v$  in terms of the model parameters in the logarithmic model:  $\epsilon$  and  $z_0$ . So based on this comparison between the logarithmic model and the  $S, A_v$  model can furthermore be concluded that there are two basic degrees of freedom to choose  $S$  and  $A_v$  left, here expressed as  $\epsilon$  and  $z_0$ . One might argue that these two degrees of freedom are restricted, however these restrictions are the result of a calibration of the  $S, A_v$ -model with a logarithmic model. Boundaries limiting the physical realistic values of  $\hat{S}, E_v$  will certainly be different if the  $S, A_v$ -model is calibrated using another turbulence closure scheme than the one used in this note.

The results of the steady flow case are used to estimate the model parameters in the tidal morphological model. For two cases the prediction of the model and the local bed structure are compared and show good agreement. This indicates that it is worthwhile to continue this line of validation.

**Acknowledgements** The author thanks H.J. De Vriend and H.E. De Swart for the ideas and discussions which have led to this paper. This note is based on work both in the PACE-project, in the framework of the EU-sponsored Marine Science and Technology Programme (MAST-III), under contract no. MAS3-CT95-0002, as well as the project of The UK Ministry of Agriculture, Fisheries and Food under contract no. CSA3051-Offshore sand banks: Basic processes and effects on long-term coastal morphodynamics.

## References

- Hulscher, S. J. M. H., Tidal-induced large-scale regular bed form patterns in a three-dimensional shallow water model, *Journ. of Geoph. Res* Vol 101 No C9, 20,727-20,744, 1996.
- Mei, C.C., *The applied dynamics of ocean surface waves*. World Scientific, 740pp, 1989.

- Off, T., Rhythmic linear sand bodies caused by tidal currents, *Bull. of the Am. Ass. of Petroleum Geologists* 47, 324-341, 1963.
- Soulsby, R. L., Tidal-current boundary layers, in *The Sea, Vol. 9. Part A*, edited by le Mehaute, B. and Hanes, D. M., pp 523- 566, Ocean Engineering Science, John Wiley and Sons, New York, 1990.
- Van Goor, S. and Andorka Gal, J.H., Bodem (in Dutch), document RIKZ/OS-96.109X, 28 pp, 1996.
- Vincent, C. and Stolk, A., Hydrodynamics and suspended load: measurements by total sediment-load sampler and acoustic backscatter, in *Sediment Mobility and Morphodynamics of the Middelkerke Bank*, edited by De Moor, G., and Lanckneus, J., pp 211-227, Final Report MAST Project, Gent, 1993.
- Zimmerman, J.T.F., On the Lorentz linearization of a quadratically damped forced oscillator, *Phys. Lett.* 89A, 123-124, 1982.